SEMARAK ILMU PUBLISHING

Journal of Advanced Research in Fluid Mechanics and Thermal Sciences

Journal homepage:
https://semarakilmu.com.my/journals/index.php/fluid_mechanics_thermal_sciences/index
ISSN: 2289-7879

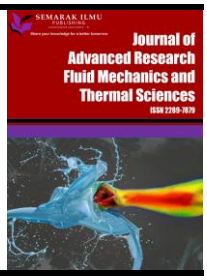

Experiment and Numerical Studies of the Effect of Equivalent Ratio on Combustion Characteristics in Fluidized Bed Gasifier

Wasu Suksuwan[1], Mohd Faizal Mohideen Batcha[2], Arkom Palamanit[3], Makatar Wae-hayee[1,*]

[1] Department of Mechanical and Mechatronics Engineering, Faculty of Engineering, Prince of Songkla University, Hatyai, Songkhla 90112, Thailand
[2] Center for Energy and Industrial Environment Studies, Universiti Tun Hussein Onn Malaysia, 86400 Parit Raja, Johor, Malaysia
[3] Energy Technology Program, Department of Specialized Engineering, Faculty of Engineering, Prince of Songkla University, Hat Yai, Songkhla 90110, Thailand

ARTICLE INFO

Article history:
Received 30 January 2023
Received in revised form 14 May 2023
Accepted 21 May 2023
Available online 8 June 2023

Keywords:
Fluidized bed; combustion; gas composition; CFD

ABSTRACT

The effect of equivalent ratio on fluidized bed gasifier on using kernel mixed palm cake as feedstock was studied experimentally and numerically. A 3-D numerical model of the reactor, similar to the experimental setup, was created using the commercial computational fluid dynamics (CFD) software ANSYS 2019 (Fluent). The fuel feed rate was fixed at 3 kg/hour and the mass flow rate of the air was varied, setting it to equivalent ratios (ER) of 0.1, 0.3, 0.5, and 0.7. The axial temperature profile in the reactor was compared between experimental measurements and numerical simulations and a good agreement was found. Carbon monoxide and volatiles increased when the equivalent ratio decreased, according to the simulations. It was found that ER = 0.1 and ER = 0.3 are suitable equivalent ratios, although the former would not give continuous combustion due to too low reactor temperature.

1. Introduction

Gasification [1,2] is an important method that converts solid fuel into fuel gas with limited air supply. The gasification encompasses four different processes in the reactor [3,4], namely drying, pyrolysis, combustion or oxidation, and gasification or reduction. The product gas [5,6] can be divided into (1) combustible gases like carbon monoxide, hydrogen, and methane; and (2) incombustible gases such as carbon dioxide, nitrogen and steam. The concentrations of combustible and incombustible gases depend on the gasifier type, the mass flow rate of air, and the feed rate of feedstock, gasification agent, other operating conditions, and solid fuel type [7-9].

According to Basu [5] there are three types of gasifier reactors, namely the fixed bed gasifier, the fluidized bed gasifier, and the entrained bed gasifier, shown in Figure 1. These differ in air flow pattern, size of solid fuel, and required product. The fixed bed gasifiers [10,11] are widely used in households, small boilers, etc. An advantage of the fixed bed gasifier is its relatively small size and

* *Corresponding author.*
E-mail address: wmakatar@eng.psu.ac.th

https://doi.org/10.37934/arfmts.106.2.167176

simplicity of design. A disadvantage, however, is the limitation on the size of solid fuel. The fluidized bed gasifier [12,13] can combust fine grained solid fuels as powder. It is applied in medium and large industrial scales in biomass power plants, waste incineration plants, cement manufacturing plants etc. However, the design is more complex and requires a larger investment than a fixed bed gasifier. In the entrained flow gasification shown in Figure 1(c), oxygen and steam are mixed with the fuel that enters the gasifier. This is different from many other types of gasifier [14]. This type has the ability to handle practically various types of feedstock and produce a clean and tar-free syngas. In addition, fine coal powder can be fed to the gasifier in either dry or slurry form.

An advantage of a fluidized bed gasifier [15-17] is that it can be designed for a wide range of feedstocks and operating conditions. In addition, it is also suitable for small to medium sized reactors in community enterprises or small scale industries. Therefore, fluidized bed gasifier was the focus of this study.

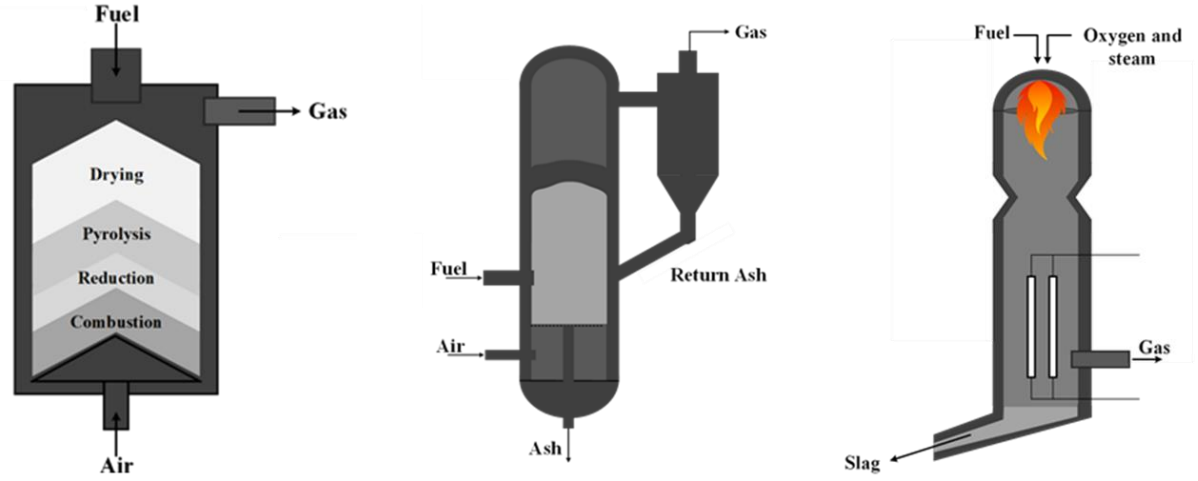

(a) Fixed bed gasifier (b) Fluidized bed gasifier (c) Entrained bed gasifier

Fig. 1. The most common gasifier types [18]

In this work, the fluidized bed gasifier was studied experimentally and numerically for several equivalent ratios [19]. Kernel mixed palm cake was applied as the feedstock. It is a by-product of agriculture from a palm oil mill [20]. A 3-D numerical model was created using the commercial CFD package ANSYS 2019 - Fluent. The main objective was to compare the experimental and the numerical results. The effects of equivalent ratio on temperature profile along the axial direction in the reactor were the main concern in this study. In addition, the gas composition and swirling flow pattern inside the reactor were also investigated from the simulation results.

2. Experimental Model

Figure 2 shows the experimental apparatus. The diameter of reactor was 20 cm, and its height was 150 cm. The air inlet of fluidized bed reactor was tangential comprising a double inlet with an inner diameter of 46.8 mm.

Air supplied by a blower was regulated using an orifice flow meter and introduced into the reactor through the double inlet. The feedstock was fed into the reactor by using a screw conveyor. The mass feed rate was controlled by changing the speed of the drive motor using an inverter. The equivalent ratios tested for gasification were 0.1, 0.3, 0.5, and 0.7.

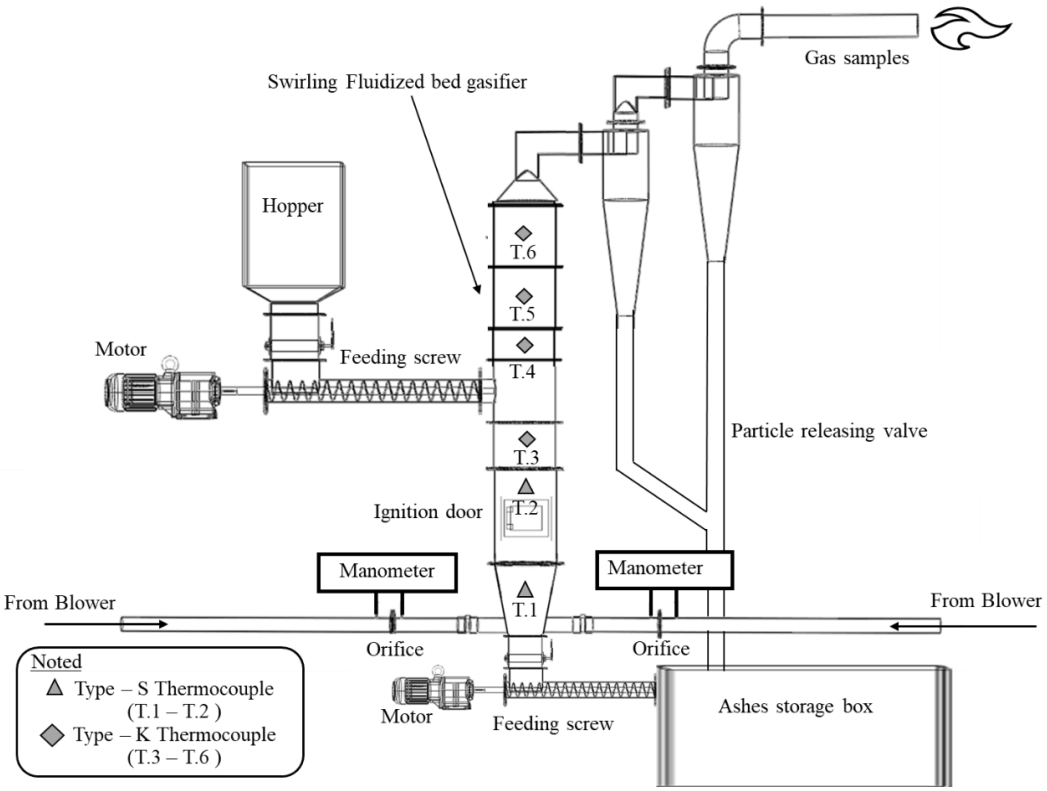

Fig. 2. Schematic diagram of swirling fluidized bed gasifier

The gasification process was started by using gasoline as igniter fuel to initiate combustion in the reactor. The gasification started immediately upon combustion of the gasoline. The product of gasification flowed to the cyclone where the syngas was separated from tar and ash.

Temperature along the reactor was recorded every minute by a data logger from S-type and K-type thermocouples. Type S thermocouples were used in the bottom part of the reactor (T.1 and T.2) due to the higher temperatures at this location, followed by K-type thermocouples (T.3, T.4, T.5, and T.6.) in the upper part of the reactor. A high temperature insulation layer (KAOWOOL, ASK-7912-H 8P Blanket 1,400 ^{o}C) was installed around the reactor to reduce heat losses.

The feedstock was kernel mixed palm cake received from a palm oil mill. The size of feedstock was less than 10 mm, approximately. Table 1 shows the ultimate analysis and proximate analysis of kernel mixed palm cake [18], which were evaluated by using CHNS/0-2000 and MACEO TGA at Scientific Equipment Center, Prince of Songkhla University.

Table 1
The properties of kernel mixed palm cake used in this work [18]

Parameter	Unit	Evaluated	Value
Ultimate analysis			
Carbon (As received basic)	% wt.	CHNS/0 Analyzer	47.01
Hydrogen (As received basic)	% wt.	CHNS/0 Analyzer	6.20
Nitrogen (As received basic)	% wt.	CHNS/0 Analyzer	1.17
Oxygen (As received basic)	% wt.	CHNS/0 Analyzer	39.18
Sulfur (As dried basic)	% wt.	CHNS/0 Analyzer	0.16
Proximate analysis			
Moisture content (As received basic)	% wt.	ASTM D7582	6.12
Fixed carbon (As received basic)	% wt.	ASTM D7582	17.67
Volatile matter (As received basic)	% wt.	ASTM D7582	70.61
Ash (As received basic)	% wt.	ASTM D7582	5.60

Experimental run parameters are shown in Table 2. The feed rate of kernel mixed palm cake was fixed at 3 kg/hour, and the mass flow rate of air was varied to the equivalent ratios (ER) 0.1, 0.3, 0.5, and 0.7. The inlet air velocities for these equivalent ratios are also shown in Table 2.

Table 2
Experimental parameters

Equivalent Ratio (ER)	Velocity of air inlet (m/s)
0.1	0.123
0.3	0.369
0.5	0.615
0.7	0.961

3. Numerical Simulation Model

3.1 Computational Model and Grid Generation

The 3-D model of fluidized bed gasifier was created as shown in Figure 3, by using the commercial CFD software ANSYS 2019 (Fluent). The size of domain was similar to the experimental gasifier. The four boundary conditions are summarized in Table 3.

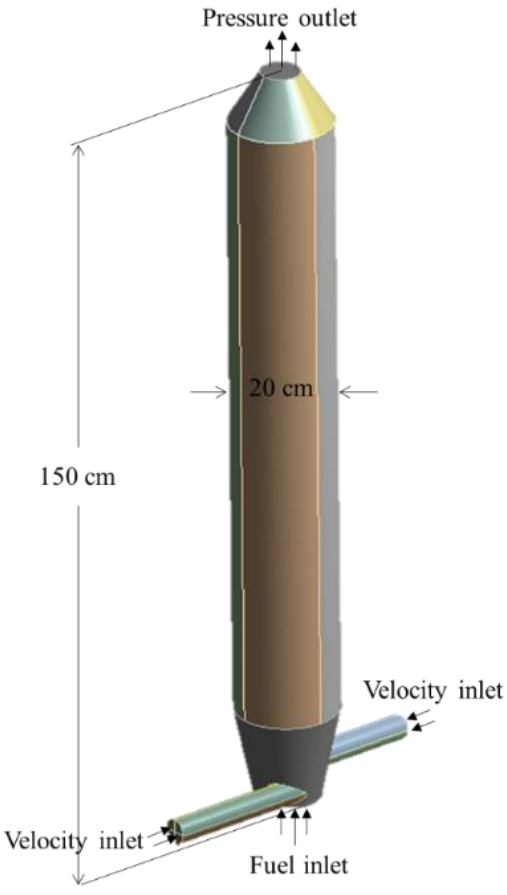

Fig. 3. Computational model and its boundary conditions

Table 3
The details of boundary conditions

Boundary at	Specified
Air inlet	Velocity at inlet (From Table 2)
Air outlet	Pressure at outlet (1 atm)
Fuel inlet	Fuel rate (3 kg/hr)
Surfaces of reactor	Solid walls

Figure 4 shows the grid generated for the domain of fluidized bed, which was mostly designed as a rectangular grid. The grid was adjusted in some areas dependent on velocity of the air. In this work, the generated grid had 1.93 million elements based on a grid size dependency test in our previous study [21].

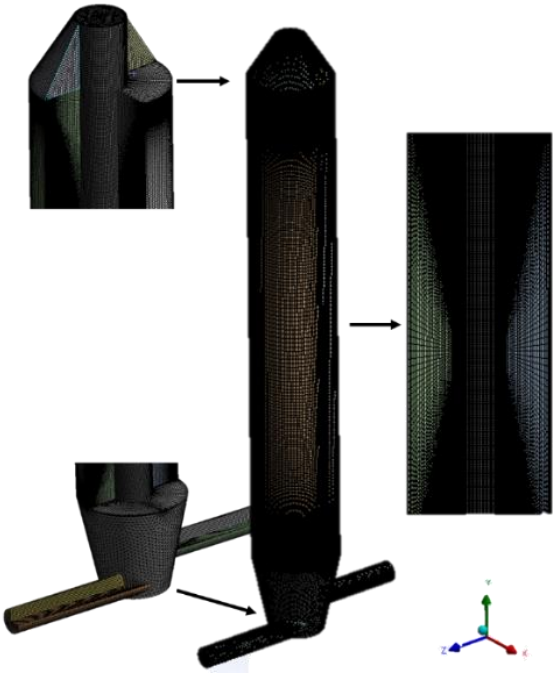

Fig. 4. Generated rectangular grid for the numerical model

3.2 Calculation Method and Algorithm

Computations were conducted by solving Reynolds averaged continuity and Navier-Stokes equations under existing boundary conditions. K-epsilon model as the viscous model was adopted here, as it typically performs well for an internal flow, with a moderate computational cost. The radiation model used in this work was Discrete Ordinate (DO) model. The species transport model used was based on the proximate analysis and the ultimate analysis of kernel mixed palm cake.

The SIMPLE algorithm used had an upwind scheme, actually separated to two upwind schemes. The first order upwind scheme was used for turbulent kinetic energy and turbulent dissipation rate as well as for discrete ordinates. The second order upwind scheme was used for pressure, momentum, volatiles, CO_2, H_2O, CO, and energy. The iterative solution was converged when the residuals of all variables were less than 1×10^{-4}.

4. Results

4.1 Visual Observations of Flame During Experiment

The photo of incombustible gas and the flame of combustible gases during testing are shown in Figure 5. For Figure 5(a), it can be seen that the incombustible gas was produced when direct combustion occurs at a higher mass flow rate of air. The gas color was grey-white as seen in the figure. The flame produced by syngas firing is shown in Figure 5(b), with the flame starting from the pipe outlet. The flame was continuous due to constant production of the combustible gases CO, H2 and CH4.

Thus, gasification was confirmed as consistent with the flame of combustible gas (Figure 5(b)) and with incombustible syngas (Figure 5(a)). Direct near complete combustion took place at ER = 0.7. In contrast ER = 0.3 gave the most combustible gas for continuous combustion. Cases ER = 0.7 and ER = 0.1 did not give continuous ignition due to the lower amount of combustible syngas.

(a) Incombustible gas (ER = 0.7) (b) flame of combustible gas (ER = 0.3)

Fig. 5. Photo of incombustible gas and flame of combustible gas

4.2 Experimental and Simulated Temperature Profiles

Figure 6 shows the temperature profiles and temperature contour along the fluidized bed gasifier observed experimentally and from numerical simulations. The six experimentally observed temperatures were measured at H = 0.25, 0.55, 0.65, 0.95, 1.10, and 1.25 m and were compared with the numerical results.

The numerical results were generally similar to the experimental observations. Firstly, the temperatures were similar throughout the reactor at equivalent ratios ER = 0.3 (Figure 6(b)) and ER = 0.5 (Figure 6(c)). The maximal temperature in ER = 0.3 case was at 0.24 m height experimentally and at 0.28 m from simulation, which are very closely similar. In case ER = 0.5, the maximum temperature from simulation was at H = 0.15 m which is a lower height than the positions that were measured experimentally (H = 0.25 m was the lowest position of thermocouple).

Secondly, consider the equivalent ratio 0.1 (Figure 6(a)). The experimental and numerical temperature profiles clearly differ. The ER = 0.1 case had the lowest temperatures because of its lowest mass flow rate of air, and the combustion was not continuous. Experimentally ER = 0.1 at H = 0.25 m had the maximum temperature of 850 °C, because of direct combustion in a small zone along the height of the reactor, and further upwards the temperature then was very low when compared to the other equivalent ratios. The simulation gave below 300 °C temperatures at all points along the reactor because no proper combustion was taking place.

The last case is ER = 0.7 (Figure 6(d)). The experimental results were similar to the numerical results at starting point (H = 0.25 cm) and ending point (H=1.25 cm). Furthermore, the highest temperature occurred at 0.32 m height, namely 1,800 °C from the simulation. The experimental and

simulated temperatures in this case differed significantly from H = 0.3 m to H = 1.1 m, giving a poorer match than at the lower equivalent ratios.

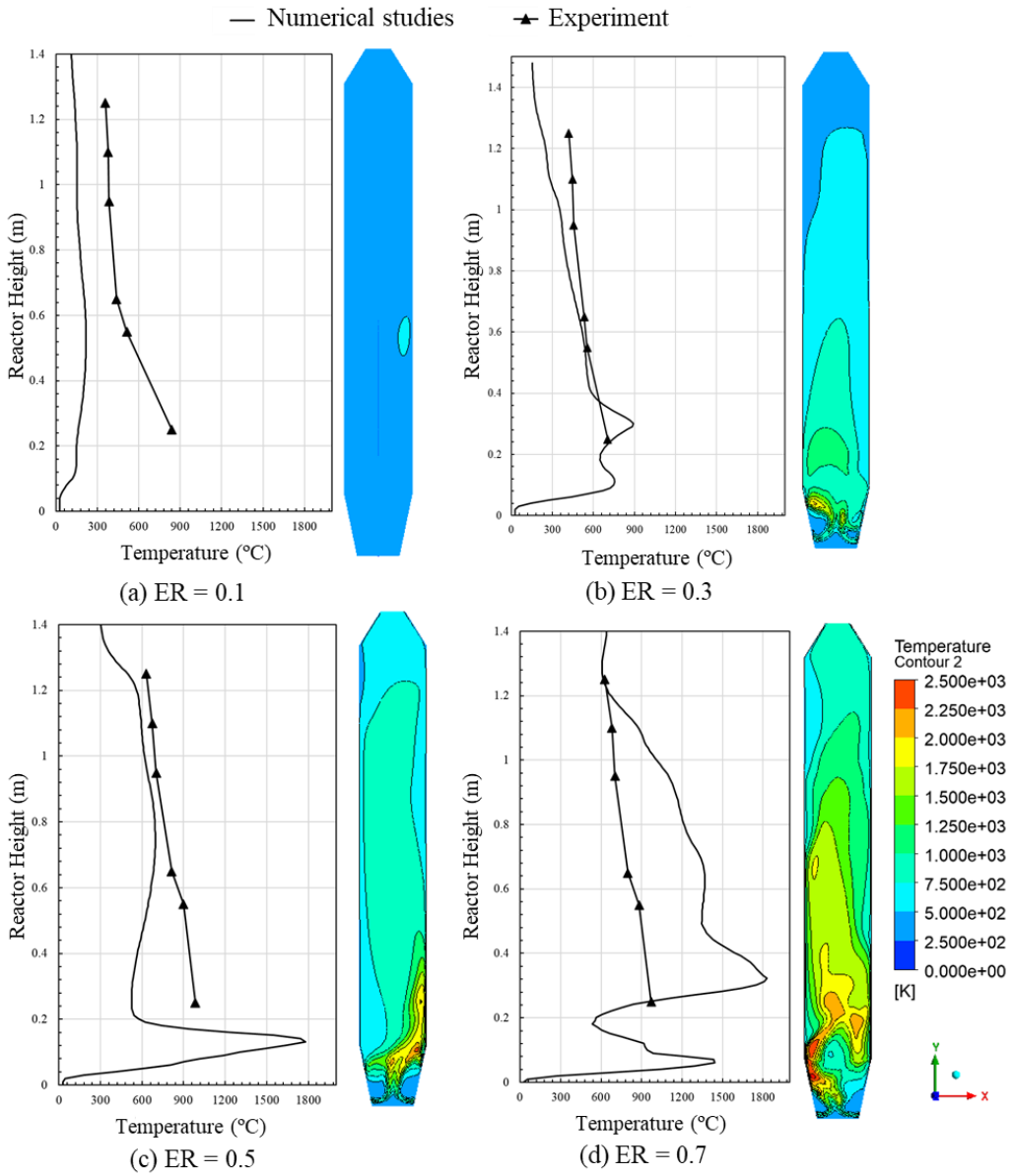

Fig. 6. The temperature profiles along the reactor

4.3 The Effect of Angle of Attack

The gas composition at constant pressure outlet is compared between the various equivalent ratios in Figure 7. The combustible gases, carbon monoxide and volatiles, are shown in red color, while the incombustible gases (carbon dioxide, water, nitrogen, and oxygen) are shown in black color.

It was found that the production of combustible gases decreased with equivalent ratio, while the content of incombustible gases increased. In addition, the oxygen mass fraction was practically at zero in all cases, because none of these equivalent ratios was not sufficient for complete combustion. So, it can be seen that the best equivalent ratios for gasification were ER 0.1 and 0.3, among the cases tested. However, the case ER = 0.1 did not allow continuous gasification. The higher equivalent ratios

than 0.3 gave direct combustion instead of gasification with fuel gas product. In summary ER = 0.3 is the preferred choice among the cases tested.

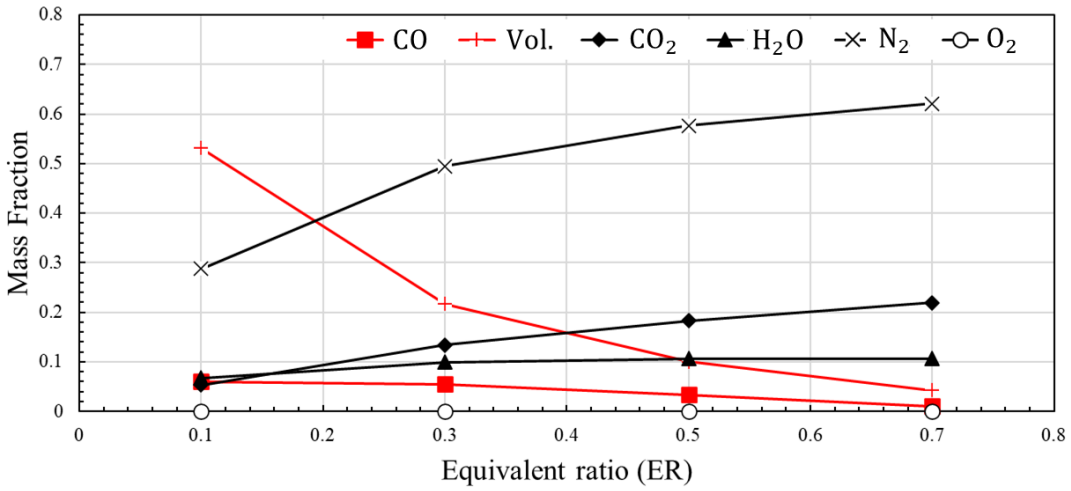

Fig. 7. The gas compositions from simulations

4.4 Flow Characteristics In Reactor From Simulations

Figure 8 shows the u-component of velocity (parallel to X-axis) along the fluidized bed gasifier at heights from 0.15 to 0.35 m measured from the bottom, from the numerical simulations. The tangential air inlet was fed at H = 0.15 m from the bottom. A swirling flow pattern in the fluidized bed gasifier during combustion is observed. The results show that the u-component of velocity at H = 0.15 m for ER = 0.1, 0.3, and 0.5 was symmetric across the X-axis. In the ER = 0.7 case, the u-component of velocity was highest in the middle. At H = 0.25 m, the u-component of velocity was symmetric at ER = 0.3. The other conditions gave asymmetric flows because this level was the starting point of combustion. At H = 0.35 m, every equivalent ratio gave asymmetry because this position had the maximal reaction temperature as seen in Figure 6.

In summary, ER 0.3 was the most suitable choice for gasification in a fluidized bed gasifier, because it gave a high proportion of combustible gases in the output and allowed continuous combustion. Similar findings have been reported by Mansarat *et al.,* [22] and Makwana *et al.,* [23].

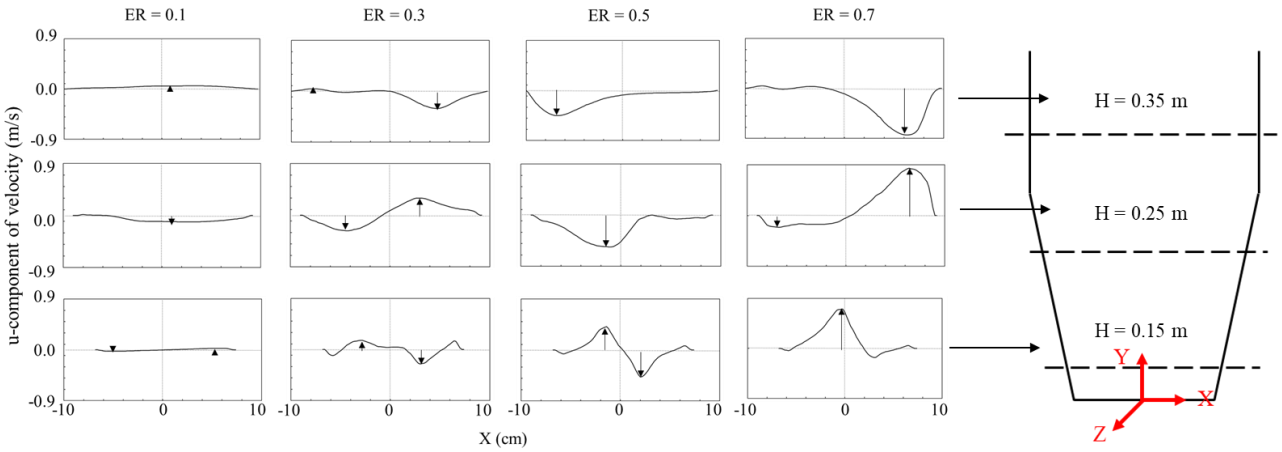

Fig. 8. The u-component of velocity on X-axis according to numerical simulations. (Arrows indicate the direction of velocity in the reactor)

5. Conclusions

In conclusion, the fluidized bed gasifier using kernel mixed palm cake as feedstock was observed experimentally and simulated numerically. The simulations and experiments matched well especially in the cases with ER = 0.3 and ER = 0.5. The proportion of combustible gases in the outflow decreased with equivalent ratio, being highest at ER = 0.1 and ER = 0.3. The former of these did not allow continuous combustion. A swirling flow pattern occurred at ER = 0.3 according to the simulations. Among the cases tested, ER = 0.3 was the most suitable choice for gasification in the fluidized bed gasifier of this study.

Acknowledgement

This work was financially supported by the Research and Development Office (RDO) of the Prince of Songkla University (PSU), Grant No. ENG 6402068S and the Graduate School of Prince of Songkla University (PSU), Thailand. Authors also thank the Energy Technology Research Unit (ETRC) of PSU for partial support to Mr. Wasu during this work. We also thank Assoc. Prof. Dr. Seppo Karrila for proofreading the manuscript via publication service of Research and Development Office (RDO), PSU.

References

[1] McAllister, S., Chen, J. Y., & Fernandez-Pello, A. C. (2011). *Fundamentals of combustion processes* (Vol. 302). New York: Springer. https://doi.org/10.1007/978-1-4419-7943-8

[2] Gnanapragasam, N. V., and M. A. Rosen. "A review of hydrogen production using coal, biomass and other solid fuels." *Biofuels* 8, no. 6 (2017): 725-745. https://doi.org/10.1080/17597269.2017.1302662

[3] Kumar, Ajay, David D. Jones, and Milford A. Hanna. "Thermochemical biomass gasification: a review of the current status of the technology." *Energies* 2, no. 3 (2009): 556-581. https://doi.org/10.3390/en20300556

[4] Parthasarathy, Prakash, Naveen Kumar Gupta, and K. Sheeba Narayanan. "Effect of composting on products of slow pyrolysis." *Biofuels* 6, no. 5-6 (2015): 313-321. https://doi.org/10.1080/17597269.2015.1110772

[5] Basu, Prabir. *Biomass gasification and pyrolysis: practical design and theory*. Academic press, 2010.

[6] Bartik, Alexander, Florian Benedikt, Andreas Lunzer, Constantin Walcher, Stefan Müller, and Hermann Hofbauer. "Thermodynamic investigation of SNG production based on dual fluidized bed gasification of biogenic residues." *Biomass Conversion and Biorefinery* 11, no. 1 (2021): 95-110. https://doi.org/10.1007/s13399-020-00910-y

[7] Mauerhofer, A. M., S. Müller, A. Bartik, F. Benedikt, J. Fuchs, M. Hammerschmid, and H. Hofbauer. "Conversion of CO2 during the DFB biomass gasification process." *Biomass Conversion and Biorefinery* 11, no. 1 (2021): 15-27. https://doi.org/10.1007/s13399-020-00822-x

[8] Vaish, Barkha, Bhavisha Sharma, Vaibhav Srivastava, Pooja Singh, M. Hakimi Ibrahim, and Rajeev Pratap Singh. "Energy recovery potential and environmental impact of gasification for municipal solid waste." *Biofuels* 10, no. 1 (2019): 87-100. https://doi.org/10.1080/17597269.2017.1368061

[9] Acharya, Bishnu, Animesh Dutta, and Prabir Basu. "Gasification of biomass in a circulating fluidized bed based calcium looping gasifier for hydrogen-enriched gas production: experimental studies." *Biofuels* 8, no. 6 (2017): 643-650. https://doi.org/10.1080/17597269.2015.1118782

[10] Chopra, Sangeeta, and Anil Jain. "A review of fixed bed gasification systems for biomass." (2007).

[11] Reed, Thomas B., and Agua Das. *Handbook of biomass downdraft gasifier engine systems*. Biomass Energy Foundation, 1988. https://doi.org/10.2172/5206099

[12] Basu, Prabir. *Combustion and gasification in fluidized beds*. CRC press, 2006. https://doi.org/10.1201/9781420005158

[13] Fuchs, Josef, J. C. Schmid, Stefan Müller, Anna Magdalena Mauerhofer, Florian Benedikt, and Hermann Hofbauer. "The impact of gasification temperature on the process characteristics of sorption enhanced reforming of biomass." *Biomass Conversion and Biorefinery* 10 (2020): 925-936. https://doi.org/10.1007/s13399-019-00439-9

[14] Phillips, Jeffrey. "Different types of gasifiers and their integration with gas turbines." *The gas turbine handbook* 1 (2006).

[15] Warnecke, Ragnar. "Gasification of biomass: comparison of fixed bed and fluidized bed gasifier." *Biomass and bioenergy* 18, no. 6 (2000): 489-497. https://doi.org/10.1016/S0961-9534(00)00009-X

[16] Breault, Ronald W. "Gasification processes old and new: a basic review of the major technologies." *Energies* 3, no. 2 (2010): 216-240. https://doi.org/10.3390/en3020216

[17] Müller, Stefan, Lara Theiss, Benjamin Fleiß, Martin Hammerschmid, Josef Fuchs, Stefan Penthor, Daniel C. Rosenfeld, Markus Lehner, and Hermann Hofbauer. "Dual fluidized bed based technologies for carbon dioxide reduction—example hot metal production." *Biomass Conversion and Biorefinery* 11 (2021): 159-168. https://doi.org/10.1007/s13399-020-01021-4

[18] Suksuwan, Wasu, Makatar Wae-hayee, and Maizirwan Mel. "Development of mini pilot fluidized bed gasifier for industrial approach: Preliminary study based on continuous operation." *Journal of Advanced Research in Fluid Mechanics and Thermal Sciences* 45, no. 1 (2018): 35-43.

[19] Li, Yanji, Huihui Wang, Wei Zhang, Rundong Li, and Yong Chi. "Study on the simulation of source-separated combustible solid waste fluidized bed gasification based on Aspen Plus." *Biofuels* 5, no. 6 (2014): 703-712. https://doi.org/10.1080/17597269.2015.1016373

[20] John, Inyang, Andrew-Munot Magdalene, Syed Shazali Syed Tarmizi, and Johnathan Tanjong Shirley. "A model to manage crude palm oil production system." In *MATEC Web of Conferences*, vol. 255, p. 02001. EDP Sciences, 2019. https://doi.org/10.1051/matecconf/201925502001

[21] Suksuwan, Wasu, Makatar Wae-hayee, and Maizirwan Mel. "The Effect of Single and Double Air Inlets on Swirling Flow in a Reactor of a Fluidized Bed Gasifier." *Journal of Advanced Research in Fluid Mechanics and Thermal Sciences* 44, no. 1 (2018): 157-166.

[22] Mansaray, K. G., A. E. Ghaly, A. M. Al-Taweel, F. Hamdullahpur, and V. I. Ugursal. "Air gasification of rice husk in a dual distributor type fluidized bed gasifier." *Biomass and bioenergy* 17, no. 4 (1999): 315-332. https://doi.org/10.1016/S0961-9534(99)00046-X

[23] Makwana, J. P., A. K. Joshi, Rajesh N. Patel, and Darshil Patel. "Effect of Equivalence Ratio on Performance of Fluidized Bed Gasifier Run with Sized Biomass." *International Journal of Energy and Power Engineering* 10, no. 6 (2016): 1059-1063.